Journal of Magnetism and Magnetic Materials 476 (2019) 483–486

Contents lists available at ScienceDirect

Journal of Magnetism and Magnetic Materials

journal homepage: www.elsevier.com/locate/jmmm

Control of the stripe domain pattern in $L1_0$-ordered FePd thin films

A. Stellhorn[a,*], A. Sarkar[a], E. Kentzinger[a], M. Waschk[a], P. Schöffmann[b], S. Schröder[a], G. Abuladze[a], Z. Fu[b], V. Pipich[b], T. Brückel[a]

[a] Forschungszentrum Jülich GmbH, Jülich Centre for Neutron Science (JCNS-2) and Peter Grünberg Institut (PGI-4), JARA-FIT, 52425 Jülich, Germany
[b] Forschungszentrum Jülich GmbH, Jülich Centre for Neutron Science at MLZ, Lichtenbergstraße 1, 85748 Garching, Germany

ARTICLE INFO

Keywords:
Neutron scattering
Magnetic depth-profile
Magnetic domains

ABSTRACT

$L1_0$-ordered FePd thin films with strong perpendicular magnetic anisotropy and self-organized domain patterns have been prepared using molecular beam epitaxy. We demonstrate reproducible growth methods for controlling the strength of the anisotropy and the lateral domain patterns. Neutron scattering experiments have been used to probe the FePd domain structure and were compared with simulations in the framework of the Distorted Wave Born Approximation.

1. Introduction

Ferromagnetic thin films with perpendicular magnetic anisotropy (PMA) have attracted much attention due to their potential application in the field of magnetic recording, logic and memory devices [1]. The most promising systems are materials/ alloys exhibiting $L1_0$-ordering and periodically arranged magnetic domain 'stripes' of alternating up and down magnetization perpendicular to the film plane [2] [Fig. 1]. To ensure the evolution of PMA during film growth, researchers have evaluated the thin film behaviour with respect to the growth temperature [3], crystallinity [4] or thickness [5].

The domain formation is strongly dependent on the strength of magnetic anisotropy in the thin film. High PMA usually leads to a 'maze' domain structure, whereas stripe domains can only be obtained at weak or low magnetic anisotropies. For films with weak PMA the in-plane magnetization component is very strong. The domains are spontaneously aligned [6] and exhibit closure domains to reduce the stray field energy [7]. Thus it is challenging to have high PMA and stripe domains in the same ferromagnetic layer, making it necessary to optimize the growth conditions to include both competing factors. In this study we present a reproducible growth method of FePd thin films with both strong PMA and stripe domains.

Magnetic force microscopy (MFM) is used to gain information about the domain pattern. The strength of PMA is verified by measuring the magnetic hysteresis at room temperature using a Quantum Design magnetic property measurement system (MPMS). To study the magnetic depth-profile, we use grazing incidence small angle neutron scattering (GISANS). Due to the coupling of the neutron spin and the magnetic induction inside the sample, it proves to be a powerful tool to analyse the depth-resolved lateral domain structure in ferromagnetic thin films [8]. The GISANS measurement was carried out at the Heinz Maier-Leibnitz Zentrum in Munich at the KWS-3 instrument.

2. Sample growth

FePd in the $L1_0$-ordered phase grows with Fe and Pd occupying alternating layers in a tetragonally distorted fcc-phase [4]. As chemical ordering in the system leads to PMA, precise and optimized growth conditions are crucial. We use state-of-the-art molecular beam epitaxy (MBE) to grow FePd films using following methods – (i) codeposition, where the Fe and Pd are simultaneously evaporated from their respective effusion cell at an elevated substrate temperature (T_s), and (ii) shuttered growth, where single Fe and Pd layers are deposited by alternatingly closing the shutter of respective effusion cells with a constant evaporation time at room temperature.

High quality epitaxial thin films were grown on MgO(001) substrate under ultra-high vacuum (base pressure of 10^{-10} mbar). To reduce the lattice misfit and ensure an epitaxial growth, first a Cr seed layer (~1 nm) is grown at room temperature on MgO(001) substrate, followed by a Pd buffer layer (~60 nm) and then heated to 723 K for 30 min. After the growth of the FePd layer, a thin capping layer (2–5 nm) of either Pd or Nb is deposited to prevent surface oxidation.

For the study, three samples (S1, S2, and S3) were prepared with varying growth methods (codepositon and shuttered growth) of the FePd layer. In sample S1, a 54 nm thick FePd layer was codeposited at T_s = 500 K with a deposition rate of ~0.2 Å/s. Sample S2 consists of a 37 nm FePd layer grown by shuttered growth at T_s = 300 K. Sample S3 is a bilayer structure where both growth methods are combined: First a

* Corresponding author.
E-mail address: a.stellhorn@fz-juelich.de (A. Stellhorn).

https://doi.org/10.1016/j.jmmm.2018.12.059
Received 30 August 2018; Received in revised form 6 December 2018; Accepted 14 December 2018
Available online 15 December 2018

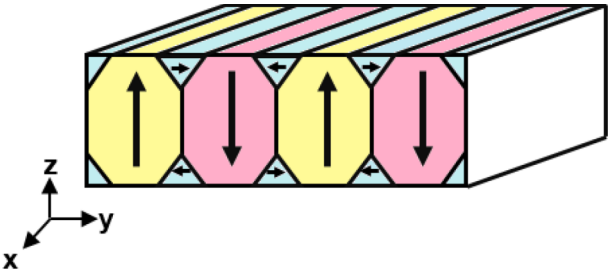

Fig. 1. Schematics of a ferromagnetic thin film with low magnetocrystalline anisotropy in z-direction and closure domains on the surfaces.

36 nm thick FePd layer is grown by shuttered growth at room temperature, followed by a second layer of 34 nm grown by codeposition at T_s = 500 K. The layer thicknesses were measured and calibrated using X-ray reflectometry (XRR) measurements. X-ray diffractometry was used to evaluate the long-range ordering of the FePd films [9]. It is observed that (a) S1 has highest degree of structural ordering, (b) S2 has no long range ordering, and (c) S3 shows moderate long-range ordering.

3. Magnetization analysis

Fig. 2 shows the hysteresis loops of the three samples where the magnetization M is plotted as a function of the applied field H. It is observed that S1 has a strong PMA along ⟨001⟩-direction, whereas S2 has a strong in-plane anisotropy. However, in S3 the ⟨001⟩-direction still denotes the easy axis but with a higher in-plane component than in S1.

Due to the different strength of magnetocrystalline anisotropy of the three samples, we need to consider the effective uniaxial anisotropy constant K_{eff} as the sum of the magnetocrystalline and the shape anisotropy constants $K_{eff} = K_u + K_{sh}$. K_{eff} can be obtained from Fig. 2 as the integral over the difference from the out-of-plane and the in-plane hysteresis loops [10]:

$$K_{eff} = K_u - \frac{1}{2}\mu_0 M_s^2 = \int_0^{M_s} (H_\perp - H_{||}) dM, \quad (1)$$

where M_s is given in [A/m], $\mu_0 H_s$ in [T] and K_{eff} in [J/m^3]. From this we deduce K_u to determine the quality factor Q of the strength of PMA, which can be calculated by the ratio of K_u and the shape anisotropy constant $K_{sh} = \frac{1}{2}\mu_0 M_s^2$ [11]. For $Q > 1$ the thin film has a strong PMA, whereas $Q < 1$ denotes an in-plane easy axis of magnetization [6]. The Q-values and K_u for the three samples are listed in Table 1.

Fig. 3 shows the MFM images of the three as grown samples. The strong PMA in S1 (Q = 2.17) results in a maze domain structure as there is no preferred in-plane orientation [Fig. 3(a)]. S2 exhibits a high in-plane magnetization component with $Q < 1$ forming stripe domains [Fig. 3(b)]. Interestingly, S3 has both – high Q value and a parallelly aligned domain structure [Fig. 3(c)]. This can be explained by considering that the two FePd layers of S3 are in direct contact to each other and exhibit a magnetic coupling between them. We assume that the domain alignment of the first shuttered layer acts as a seed for parallelly aligned domain formation in the codeposited layer. The domain thicknesses are obtained from the MFM measurements to be 75 nm, 49 nm and 59 nm for samples S1, S2 and S3, respectively.

Table 1
K_u and Q-values of the samples obtained from the hysteresis loop measurements.

Parameters	S1	S2	S3
K_u [kJ/m^3]	1362	326	1241
Q	2.17	0.47	1.46

The domain structure of samples S2 and S3 can be manipulated by applying an external magnetic field higher than the out-of-plane saturating field. Fig. 4(a) shows the MFM image of the as-grown sample S3, Fig. 4(b) the measurement after treatment in 700 mT in out of plane magnetic field. However, the parallel domain formation can be retrieved (with some structural defects) [Fig. 4(c)] by demagnetizing the sample with an in-plane oscillating magnetic field parallel to the initial stripe formation. For S2 the same behaviour can be observed after treating the sample with this procedure. The behaviour of magnetic domains with weak PMA to align spontaneously is referred to a high exchange anisotropy energy and is described elsewhere [6,11].

4. Neutron scattering

For the GISANS measurement we used a $Pd_{1\,nm}/FePd_{39\,nm}/Pd_{47\,nm}/Cr_{2\,nm}$ heterostructure on MgO(001) substrate. A Q-value of Q = 1.8 was obtained from the magnetization measurements, which is in between the Q-values of S1 and S3. MFM measurements show a parallel configuration of the magnetic domains in the as grown state of the sample as obtained for S3. We measure the scattering intensities as a function of the scattering wave vectors Q_y and Q_z with z in the out-of-plane and y in the in-plane direction of the sample [Fig. 5(d)]. Due to a periodic arrangement of the magnetic domains in y-direction with periodicity w, scattering peaks can be observed at $Q_y = 2\pi/w$. For the measurements we used a sample to detector distance of d_{sd} = 1.23 m and a wavelength λ = 12.8 Å with a wavelength spread of $\Delta\lambda/\lambda$ = 17%. The measurement was performed at 300 K with no applied external magnetic field. To probe the magnetic domain pattern, the sample was aligned such that the incoming wave vector of the neutrons has mainly a component along the x-direction and a small component in the z-direction.

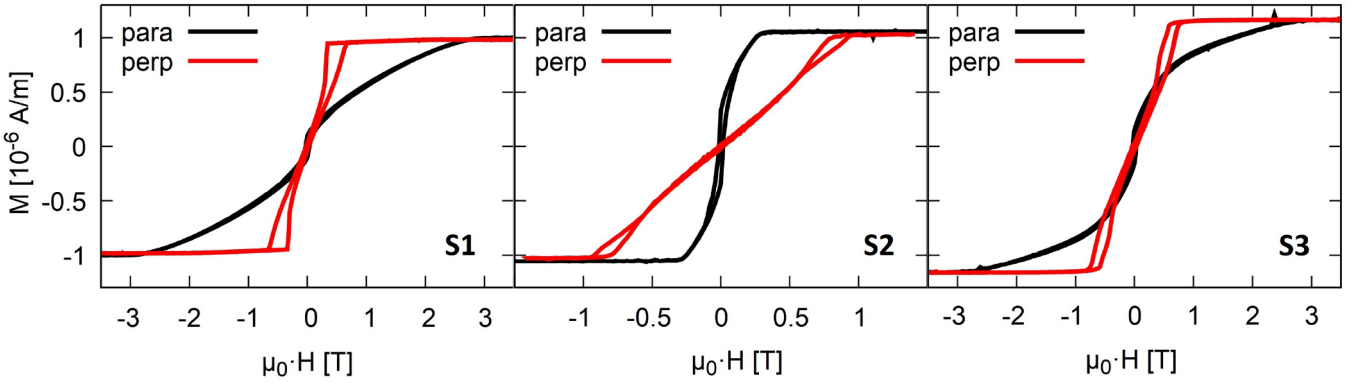

Fig. 2. Hysteresis loops of S1, S2 and S3 measured at 300 K with the external magnetic field in the surface plane ("para", measured along a ⟨100⟩ crystallographic orientation) and perpendicular to the surface plane ("perp", measured along ⟨001⟩).

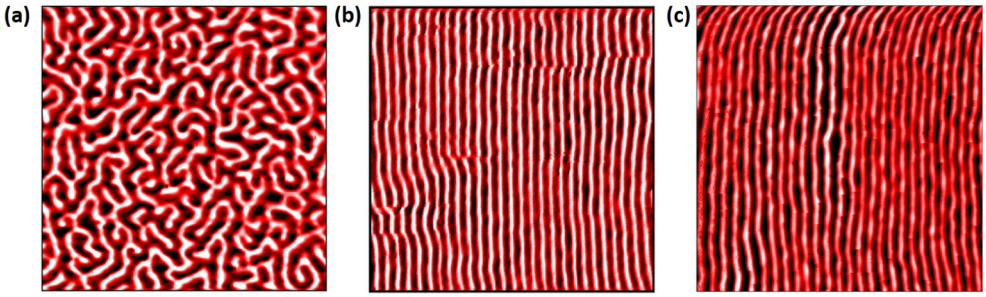

Fig. 3. $3 \times 3\,\mu$m MFM measurements in the as grown state of the three samples (a) S1, (b) S2 and (c) S3.

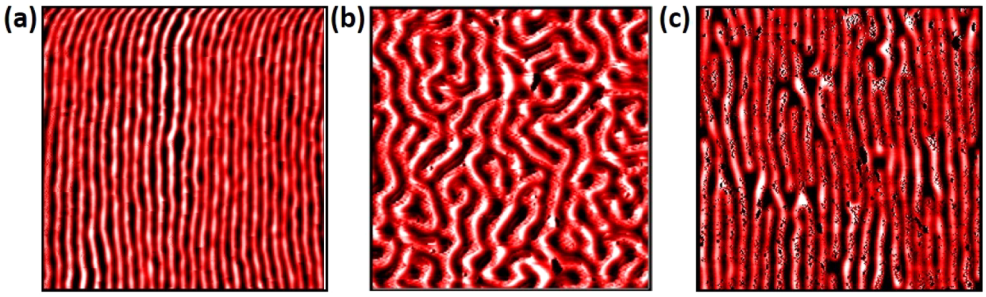

Fig. 4. $3 \times 3\,\mu$m MFM measurements at 0 applied field of S3 after applying an external magnetic field perpendicular to the sample surface of (a) 0 mT, (b) 700 mT and (c) after in-plane oscillating demagnetization.

From the resulting detector image [Fig. 5(a)] the following can be observed – (i) the specular spot at $Q_y = 0\,\mathrm{nm}^{-1}$ and $Q_z = 0.169\,\mathrm{nm}^{-1}$ with an incident angle of 0.97° and (ii) two peaks on the GISANS line with $Q_z = 0.169\,\mathrm{nm}^{-1}$ (marked by a horizontal line in Fig. 5(a) and (b)). The Q_y-Q_z-map and the intensity as function of Q_y at $Q_z = 0.169\,\mathrm{nm}^{-1}$ have been simulated using the Distorted Wave Born Approximation (DWBA)-method [12] [Fig. 5(b) and (c), respectively]. For the simulation we used a thin film heterostructure with ferromagnetic domains in $\pm z$ direction and closure domains on the FePd-layer surface as in Fig. 1. Following Navas et al. [13] the closure domains can be

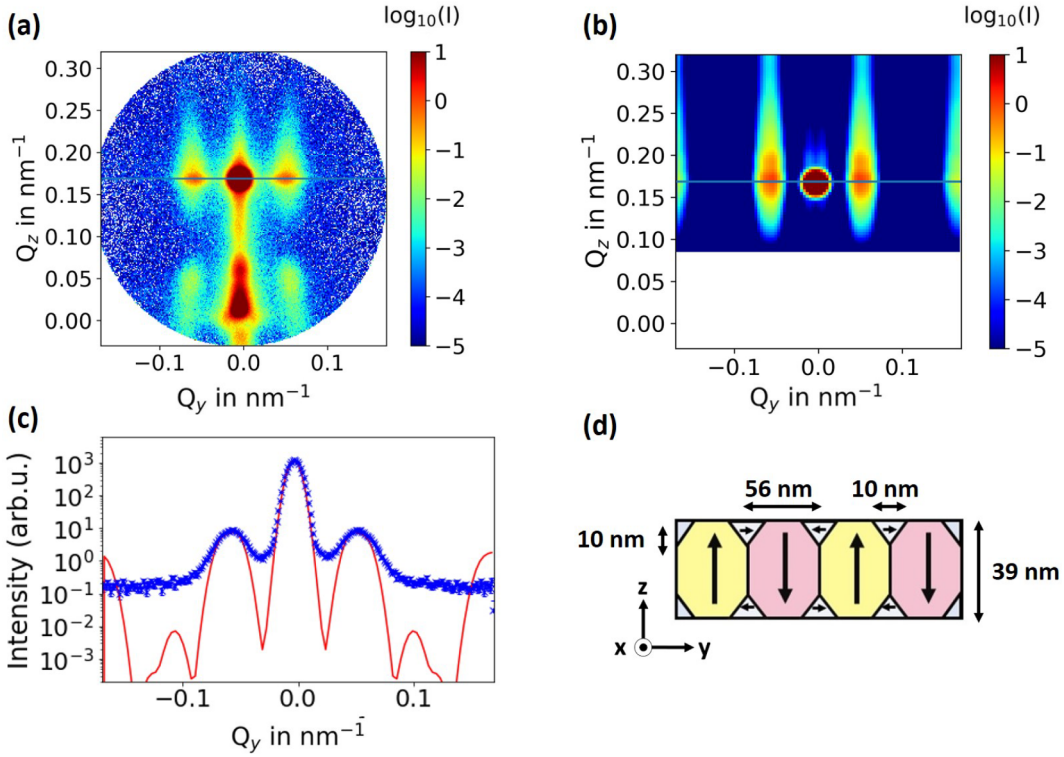

Fig. 5. (a) Q_y-Q_z scan of FePd with parallelly aligned magnetic domains. (b) Simulation of the Q_y-Q_z-map using the DWBA [12]. (c) Q_y versus intensity at $Q_z = 0.169\,\mathrm{nm}^{-1}$ of the experiment (blue) and the simulation (red). (d) Simulation parameters of the magnetic domains and closure domains in the FePd-layer. (For interpretation of the references to colour in this figure legend, the reader is referred to the web version of this article.)

considered as triangles with a fixed size and depth. Bloch domain walls inside the FePd layer were not taken into account due to the high PMA. Not included in this model are correlations along the *x*-direction due to domain width fluctuations, and a constant background on the detector. Thus the scattering signals at $Q_y = 0.1\,\mathrm{nm}^{-1}$ in the measurement cannot be resolved. The simulated signals at the edge of the detected Q_y-range (third harmonic GISANS peaks) will be lowered by assuming bending and roughness effects of the magnetic domains in *y*-direction.

According to such a model, the Q_y-Q_z-map can be reproduced by assuming small closure domains (in the example in Fig. 5(b) and (c) we have used a size and depth of 10 nm of the closure domains). The FePd layer thickness was fixed to 39 nm as a result of X-ray-reflectometry measurements on this sample. From the Q_y-dependence the domain width can be calculated to $w_d = 56$ nm and is close to the values measured in MFM. Both the closure domains and the ferromagnetic domains exhibit a periodicity of 56 nm and overlap at the same Q_y-value. The results show that this model can be used to study the lateral correlations in a domain structured ferromagnet. By inserting magnetic roughness effects in this model, the scattering intensities and peak width will give more detailed information about the width and depth of closure domains. Moreover, the scattering peaks from in-plane magnetized closure domains and out-of-plane magnetized domains can be seperated using a polarized neutron beam with polarization in *z*- or *y*-direction. Also an evaluation at different incident angles will give more detailed information on the depth profile of the closure domains.

5. Summary and outlook

In this work we have shown that a combination of codeposition and shuttered growth leads to FePd layers with high PMA as well as a parallelly aligned domain formation. A pseudo-reversible manipulation of the domain pattern of high PMA FePd layers is possible after applying a saturating magnetic field in the out-of-plane direction. Neutron scattering experiments are carried out to observe the depth-profile of the lateral magnetization in the FePd layer with parallelly aligned domains and $Q = 1.8$. For the simulation a model for the FePd layer including magnetic domains in the out-of-plane direction and closure domains in the in-plane direction was used.

Our simulation of the neutron experiments provides a good fit to the experimental results. However, in the model can be improved by including correlation effects along the *x*-direction as well as roughness in the domain and closure domain widths. By this the bending of GISANS peaks towards higher Q_y shall be simulated. Also an extension of the simulation using various incident angles to vary the penetration depth of the neutron beam inside the sample will be simulated with the program BornAgain [14]. Together with a polarized neutron beam and polarization analysis, this will give more detailed information about the structure of the closure domains on the FePd layer surfaces.

References

[1] B.M. Lairson, B.M. Clemens, Enhanced magneto-optic Kerr rotation in epitaxial PtFe (001) and PtCo(001) thin films, Appl. Phys. Lett. 63 (10) (1993) 1438–1440, https://doi.org/10.1063/1.110768.

[2] G. Beutier, G. van der Laan, K. Chesnel, A. Marty, M. Belakhovsky, S.P. Collins, E. Dudzik, J.-C. Toussaint, B. Gilles, Characterization of FePd bilayers and trilayers using soft x-ray resonant magnetic scattering and micromagnetic modeling, Phy. Rev. B 71 (18) (2005), https://doi.org/10.1103/physrevb.71.184436.

[3] T.B. Massalski, H. Okamoto, Binary Alloy Phase Diagrams, ASM International Materials Park (1986).

[4] D.E. Laughlin, K. Srinivasan, M. Tanase, L. Wang, Crystallographic aspects of $L1_0$ magnetic materials, Scr. Mater. 53 (4) (2005) 383–388, https://doi.org/10.1016/j.scriptamat.2005.04.039.

[5] V. Gehanno, R. Hoffmann, Y. Samson, A. Marty, S. Auffret, In plane to out of plane magnetic reorientation transition in partially ordered FePd thin films, Eur. Phys. J. B 10 (3) (1999) 457–464, https://doi.org/10.1007/s100510050874.

[6] G. van der Laan, K. Chesnel, M. Belakhovsky, A. Marty, F. Livet, S. Collins, E. Dudzik, A. Haznar, J. Attané, Magnetic anisotropy of aligned magnetic stripe domains in FePd studied by soft x-ray resonant magnetic scattering, magnetic force microscopy and micromagnetic modeling, Superlattice Microstruct. 34 (1–2) (2003) 107–126, https://doi.org/10.1016/j.spmi.2004.01.005.

[7] H.A. Dürr, E. Dudzik, S.S. Dhesi, J.B. Goedkoop, G. van der Laan, M. Belakhovsky, C. Mocuta, A. Marty, Y. Samson, Chiral magnetic domain structures in ultrathin FePd films, Science 284 (1999) 2166–2168, https://doi.org/10.1126/science.284.5423.2166.

[8] C. Fermon, F. Ott, B. Gilles, A. Marty, A. Menelle, Y. Samson, G. Legoff, G. Francinet, Towards a 3d magnetometry by neutron reflectometry, Physica B 267–268 (1999) 162–167, https://doi.org/10.1016/s0921-4526(99)00014-9.

[9] V. Gehanno, A. Marty, B. Gilles, Y. Samson, Magnetic domains in epitaxial ordered FePd(001) thin films with perpendicular magnetic anisotropy, Phys. Rev. B 55 (18) (1997) 12552–12555, https://doi.org/10.1103/physrevb.55.12552.

[10] J.R. Skuza, C. Clavero, K. Yang, B. Wincheski, R.A. Lukaszew, Microstructural, magnetic anisotropy, and magnetic domain structure correlations in epitaxial FePd thin films with perpendicular magnetic anisotropy, IEEE Trans. Magn. 46 (6) (2010) 1886–1889, https://doi.org/10.1109/tmag.2009.2039923.

[11] V. Gehanno, Perpendicular magnetic anisotropy of epitaxial thin films of FePd ordered alloys (Ph.D. thesis), Université Joseph-Fourier – Grenoble I (1997).

[12] E. Kentzinger, U. Rücker, B. Toperverg, F. Ott, T. Brückel, Depth-resolved investigation of the lateral magnetic correlations in a gradient nanocrystalline multilayer, Phys. Rev. B 77 (10) (2008), https://doi.org/10.1103/physrevb.77.104435.

[13] D. Navas, C. Redondo, G.A.B. Confalonieri, F. Batallan, A. Devishvili, Ó. Iglesias-Freire, A. Asenjo, C.A. Ross, B.P. Toperverg, Domain-wall structure in thin films with perpendicular anisotropy: magnetic force microscopy and polarized neutron reflectometry study, Phys. Rev. B 90 (5) (2014), https://doi.org/10.1103/physrevb.90.054425.

[14] C. Durniak, M. Ganeva, G. Pospelov, W.V. Herck, J. Wuttke, D. Yurov, BornAgain - Software for simulating and fitting X-ray and neutron small-angle scattering at grazing incidence, version < 1.12.1 > (Tech. rep.), Heinz Maier-Leibnitz Centre (2018).